

PAPER • OPEN ACCESS

Numerical analysis of heat transfer in tubular type heat exchangers of transport vehicles with pulsating flow

To cite this article: A I Haibullina *et al* 2020 *IOP Conf. Ser.: Mater. Sci. Eng.* **918** 012164

View the [article online](#) for updates and enhancements.



LIVE AWARDS AND SPECIAL EVENTS

PLENARY LECTURE:
"Perovskite Solar Cells: Past 10 Years and Next 10 Years" with *Nam-Gyu Park*

LEGENDS OF BATTERY SCIENCE:
A Celebration with *M. Stanley Whittingham* and *Akira Yoshino*

PRiME 2020 • October 4-9, 2020
Hosted daily: 2000h ET & 0900h JST/KST

PRIME™
PACIFIC RIM MEETING
ON ELECTROCHEMICAL
AND SOLID STATE SCIENCE
2020

**ATTENDEES
REGISTER FOR FREE ▶**

The banner features several logos and portraits: a green 'e' logo, a circular portrait of Nam-Gyu Park, a circular portrait of M. Stanley Whittingham, a circular portrait of Akira Yoshino, and the Electrochemical Society logo. A gold coin is also visible.

Numerical analysis of heat transfer in tubular type heat exchangers of transport vehicles with pulsating flow

A I Haibullina¹, A D Savelyeva¹, A R Hayrullin¹

¹Kazan State Power Engineering University, 51 Krasnoselskaya street, Kazan, 420066, Russian Federation

E-mail: kharullin@yandex.ru

Abstract. The shell and tube heat exchangers are widely used in many engineering applications. Tubular heat exchangers can be found in the transport, power engineering, food industry and etc. Therefore, the study of the characteristics of heat transfer and hydrodynamics in tubular heat exchangers is important. In this paper, numerical analysis of a heat transfer in a staggered tube bundle with steady and asymmetrical pulsating flow studied. The transverse and streamwise spacing-to-diameter ratios of the tube bundle were 1.3. The Reynolds number Re was 1100. Numerical simulation of the flow past the tube bundle with 7 longitudinal rows was carried out by solving the incompressible Navier-Stokes equations and energy conservation equation with two different modeling strategies. The simulation was carried out with the *RNG* k - ε turbulence model with enhanced wall treatment and laminar solver. The sensitivity of the Nusselt number to the mesh parameters is noted. The effect of the number of rows of the tube on the heat transfer rate for the tube bundle with the pulsating flow also was discussed. For the pulsating flow enhancement of the heat transfer in the tube bundle dependence from the row of the tube and modeling strategy. When *RNG* k - ε turbulence model was employed the heat transfer rate of the first row is increasing by 16 %, downstream rows by 6-7 %. When laminar solver was employed the heat transfer rate of the central rows are increasing by 53 %.

1. Introduction

The tube bundle is the main element of the shell and tube heat exchanger. Therefore, the study of the characteristics of heat transfer and hydrodynamics in tube bundles is important. There are many studies, both experimental [1-3] and numerical [4-6], on this subject. However, studies are mainly devoted to a steady flow. Heat transfer studies in forced pulsating flow in the tube bundles are limited. Forced pulsating flow can be used for the enhancement of heat transfer [7]. The use of various methods of enhancement of heat transfer can lead to a reduction in the metal consumption for heat exchange equipment, reduced pumping power, and a reduced in heat carrier costs.

In works [8-11] present an experimental investigation of the flow over tube bundles in pulsating cross-flow of water. The experimental results of flow characteristics obtained for staggered, in-line, and asymmetrical tube bundles. The heat transfer of tube bundles by the external pulsation flow is not investigated. The authors suggest a possible increase in heat transfer when the external pulsating frequency approaches the natural shedding frequency. This is referred to as the lock-on or vortex resonance phenomenon. In another study [12] effect of flow pulsating on a heat transfer of a seven-row inline tube array is investigated numerically using the LES technique. It is found an increase of heat transfer of the first and the second row, due to the lock-on regime behind the first row. Heat transfer downstream cylinders are not influenced by the forced pulsation. The effect of flow pulsation



on flow characteristics and heat transfer in tube bundles experimentally investigated in papers [13-16]. It is found what heat transfer of tube bundles can increase by the external pulsation.

In mention works pulsating flow close to harmonical. Here presented new results of heat transfer variation with the number of rows in the staggered tube bundle by external asymmetrical pulsation. In this work, the Reynolds number is based on the tube diameter and gap velocity in the tube bundle. In this work, transverse and streamwise spacing-to-diameter ratios of the tube bundle were 1.3. The Reynolds number Re is based on the tube diameter was 1100. The Prandtl number Pr was 5.1. The Strohaul number Sh of pulsating flow was 0.24. The dimensionless relative amplitude A/D was 0.2, the duty cycle ψ was 0.25. In the previous works of the authors [17-19], the efficiency of asymmetric pulsations was already shown in comparison with symmetric pulsations at a Reynolds number $Re < 1000$. In these studies [17-19], the heat transfer of the central cylinder in the tube bundle was estimated for a wide range of pulsation parameters.

2. Mathematical model

The computational domain of the tube bundle and nomenclature used in this work are shown in figure 1. The transverse and streamwise spacing-to-diameter ratios of the tube bundle were $S_{T,L}/D = 1.3$. The tube diameter was $D = 0.02$ m. The domain included 7 streamwise rows of the tube. The upstream and downstream length of the tube bundle was $5.5D$ and $9.5D$ respectively. Symmetry boundary condition was set at the lines AB and CD . Constant temperature boundary condition was set at the inlet (line AC) and the tube walls, the outlet (line BD) constant pressure.

In a steady flow, constant flow velocity was set at the inlet to the computational domain. To simulate the pulsating flow at the inlet to the computational domain of the tube bundle, the dependence of the velocity on time $u(\tau)$ s was set (figure. 2). The pulsations of the velocity $u(\tau)$ corresponded to the necessary frequency f and the relative amplitude A/D of the pulsations. The pulsation frequency was found by the equation $f = 1/T$ Hz, where $T = T_1 + T_2$ the period of pulsation consisting of two half-periods. The amplitude of the pulsations was equal to the distance that the fluid passed during the time T_1 (figure 2). The duty of the pulsation was calculated as follows $\psi = T_1/T$.

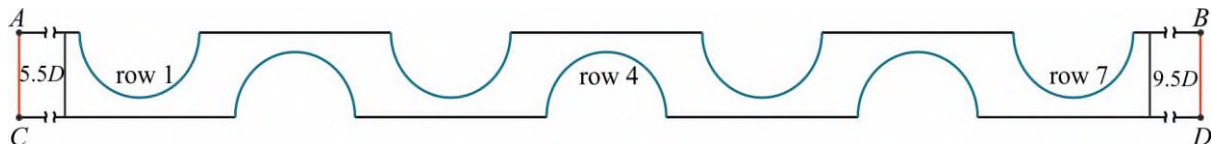


Figure 1. Computational domain.

Table 1. List of mesh parameters ordered by code.

Mesh code	Element number	y_{\min}/D	y_{\max}/D
M1	40.321	$1.56 \cdot 10^{-3}$	$1.2 \cdot 10^{-2}$
M2	65.607	$1.15 \cdot 10^{-3}$	$9.0 \cdot 10^{-3}$
M3	91.368	$8.72 \cdot 10^{-4}$	$7.5 \cdot 10^{-3}$
M4	134.074	$7.83 \cdot 10^{-4}$	$6.0 \cdot 10^{-3}$
M5	207.953	$6.31 \cdot 10^{-4}$	$4.7 \cdot 10^{-3}$

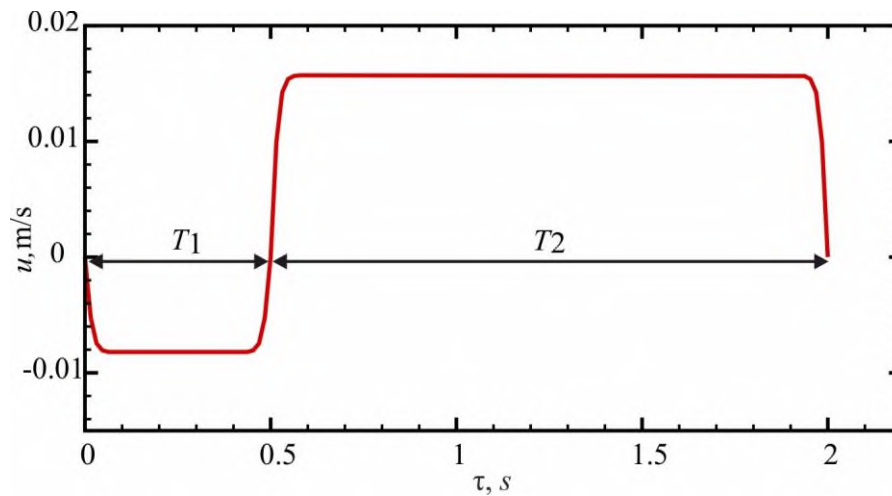


Figure 2. Asymmetrical pulsating velocity at the inlet of the tube bundle for $f = 0.5$ Hz; $A/D = 0.2$; $\psi = 0.25$; $Re = 1100$; $Pr = 5.1$.

The flow is accepted to be incompressible, $2D$, and with constant thermal properties. To simulate the flow and heat transfer in the tube bundle governing Navier–Stokes, and energy equations are solved with two different modeling strategies. The simulation was carried out with the turbulence model and laminar solver. The *RNG* $k-\varepsilon$ turbulence model with enhanced wall treatment (*RNG* $k-\varepsilon$ EWF) was employed.

The calculations were performed with the finite volume method using commercial computational fluid dynamics package Fluent [20]. The SIMPLE algorithm was used for all calculations. The energy equation is solved using the upwind scheme with second-order accuracy. The steady solver was used for the stationary flow. For pulsating flow time step was 0.001 s.

Five meshing schemes are generated for the numerical simulation. The 12 number of layers in the near-wall region with the expansion factor in the radial direction 1.2 was set. Mesh parameters information is shown in table 1. Figure 3 is shown the obtained coarse and finest mesh.

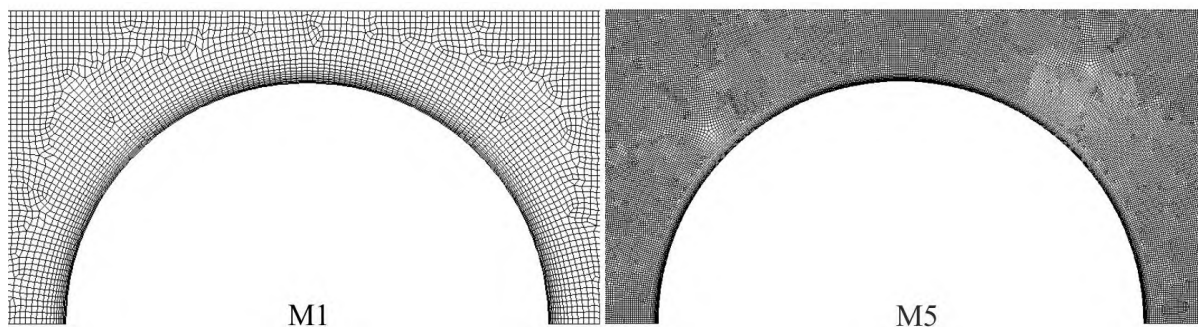


Figure 3. Details of two mesh sets.

3. Results

Figure 4–5 shows the Nusselt number Nu_{st} of steady flow obtained with five meshes and two modeling strategies. For the *RNG* $k-\varepsilon$ EWF turbulence model influence of the mesh is not significant (figure 4). Differences between the Nusselt number between M1 and M5 were below 0.42 %, between M4 and M5 below than 0.09%. The Nusselt number obtained when laminar solver was employed more sensitive to the mesh compared to the *RNG* $k-\varepsilon$ EWF turbulence model (figure 5). The sensitivity of the mesh to heat transfer varies depending on the number of rows in the tube bundle. The difference of the heat transfer for the rows 1-2 between M1 and M5 was about 0.4%, for the rows 3-7 about 3.8%. However, as the mesh decreases, the solution stabilizes. The difference between the Nusselt number

for the M4 and M5 was below 0.17%. The deviation of the obtained results with experimental data [1] was 27% and 18% for *RNG k-ε* EWF and laminar solver, respectively (Table 2).

Figure 6–7 shows the influence of the mesh on the Nusselt number Nu_p of the unsteady flow with the *RNG k-ε* EWF turbulence model and the laminar solver. In a pulsating flow, the heat transfer of the tube bundle more sensitive to the parameters of the mesh as compared to the steady flow. The difference between Nu_p between M4 and M5 was about 1.3% and 0.5% for *RNG k-ε* EWF turbulence model and the laminar solver, respectively.

When the *RNG k-ε* EWF turbulence model was employed (figure 8, (a)), the heat transfer variation with the number of the row in the tube bundle in the steady and pulsating flow is similar. The heat transfer of the second row is higher than the first row, which agrees with the data of other authors [1,4]. The heat transfer of the downstream rows is close to the heat transfer of the second row. The pulsation flow increases the heat transfer of the first row by 16% of the downstream rows by 6-7%. However, in [12], significant enhancement of the heat transfer by the external pulsation was only for the first and second row in a tube bundle. The difference can be induced by the difference in pulsation parameters, the configuration of the tube bundle, and the chosen modeling method.

When the laminar solver was employed (figure 8, (a)), the heat transfer variation with the number of the row in the tube bundle in the steady and pulsating flow is not similar. In the pulsating flow, the maximum increase of the heat transfer of the tube bundle is observed for rows 2–6, the maximum decrease of the heat transfer for the first and last rows. In the steady flow, the maximum increase of the heat transfer is observed for the second row the maximum decrease for the first and for the rows 3–7. However, the heat transfer of rows 3-7 is higher than the heat transfer of the first row. The heat transfer rate in the central rows is enhanced by 53% due to the external pulsation compare to the steady flow.

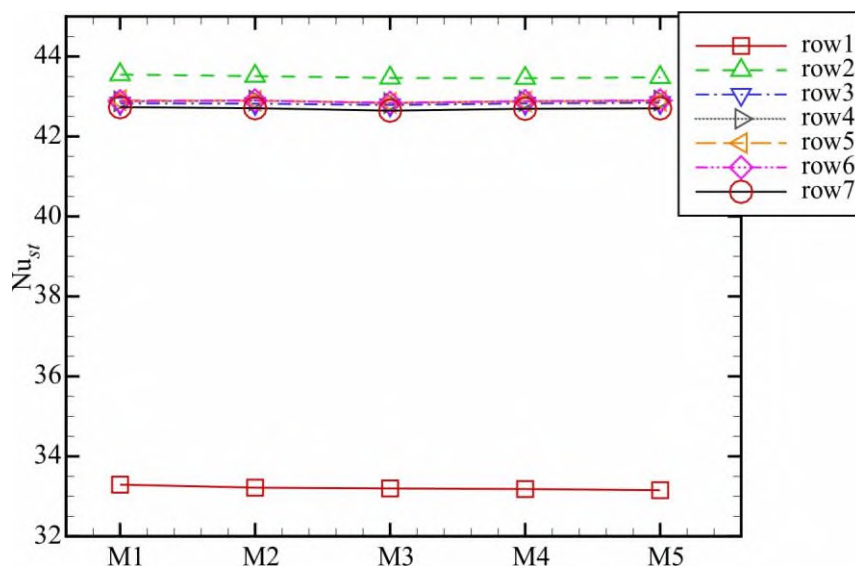


Figure 4. Nusselt number of each row in the tube bundle with different mesh for the *RNG k-ε* turbulence model (steady flow).

Table 2. Nusselt number for the second row in the bundle for verification.

Mesh code	Modeling strategy	$Nu/Pr^{0.36}$
M1	<i>RNG k-ε</i> EWF	24.22
M5	<i>RNG k-ε</i> EWF	24.19
M1	Laminar solver	22.52
M5	Laminar solver	22.54
-	Zukauskas [1] exp. data	19.1

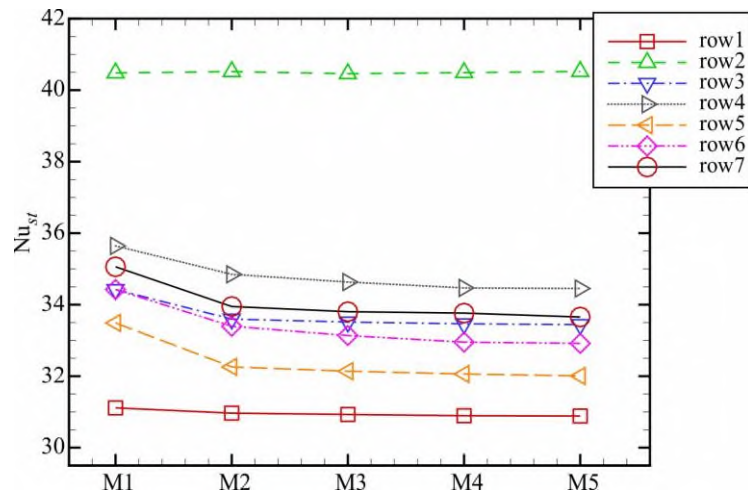


Figure 5. Nusselt number of each row in the tube bundle with different mesh for the laminar solver (steady flow).

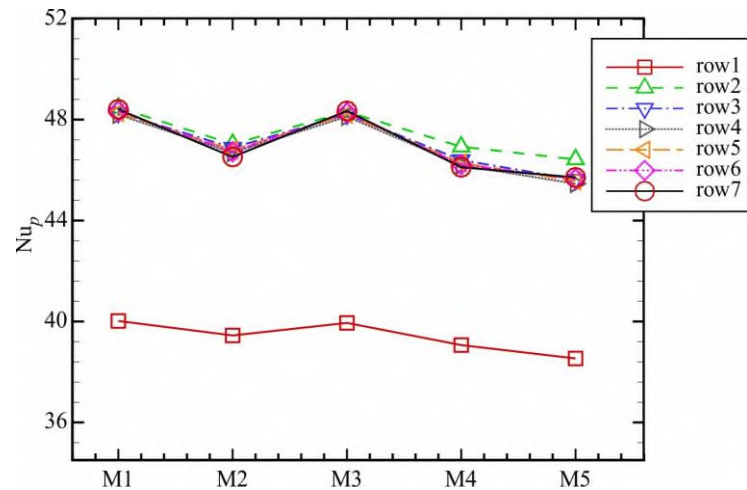


Figure 6. Nusselt number of each row in the tube bundle with different mesh for the *RNG k-ε* turbulence model (pulsating flow).

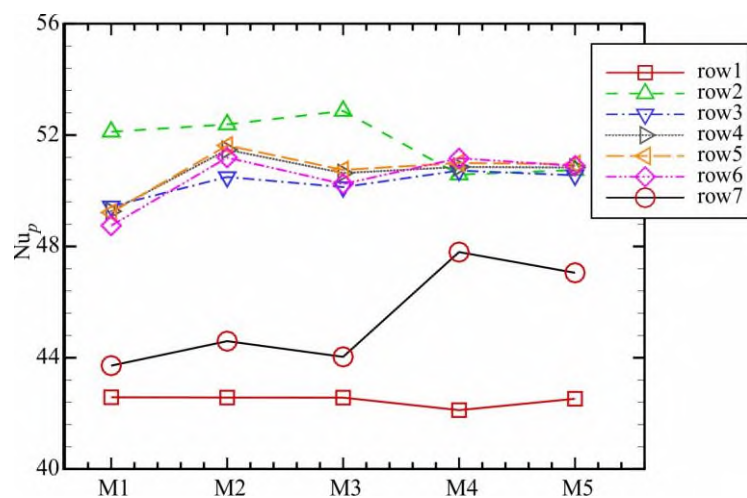


Figure 7. Nusselt number of each row in the tube bundle with different mesh for the laminar solver (pulsating flow).

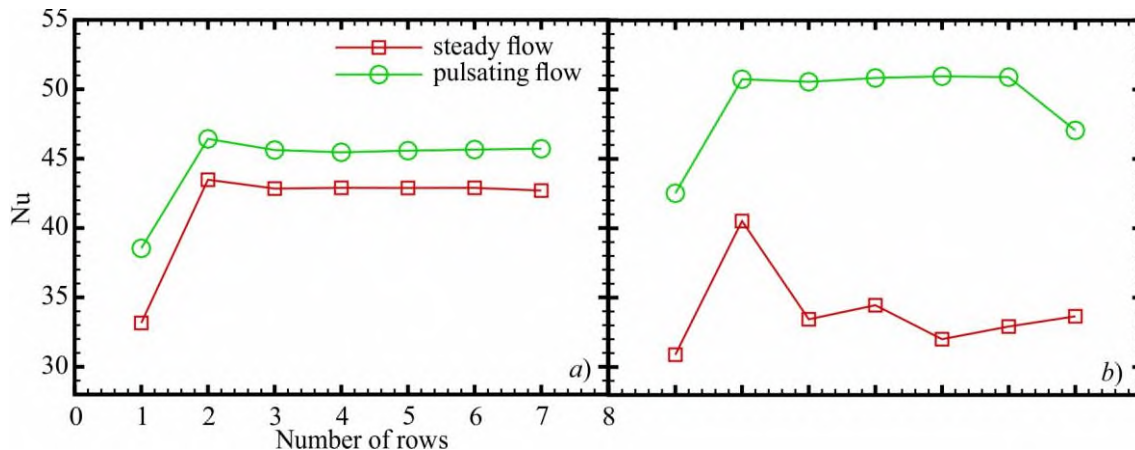


Figure 8. Nusselt number of each row in the tube bundle: a) RNG k - ε EWF turbulence model; b) laminar solver.

4. Conclusion

The RNG k - ε EWF turbulence model with enhanced wall treatment and laminar solver is employed for the numerical simulation of the flow inside a seven-row staggered tube bundle with the asymmetrical pulsating and steady flow at the inlet. It is noted that the Nusselt number obtained for pulsating flow more sensitive to the parameters of mesh compared to the steady flow. The results obtained by the two modeling strategies for the steady flow have no significant differences. The Nusselt number for the first tube in the array is lower than downstream cylinders. Differences between the two modeling strategies are more significant with pulsating flow. In the pulsating flow with the RNG k - ε EWF turbulence model, the heat transfer rate of the first row is increasing by 16 %, downstream rows by 6-7 %. When laminar solver was employed the heat transfer rate of the central rows are increasing by 53 %. It seems the laminar solver over predict the heat transfer in the tube bundle with the pulsating flow. The further experimental investigation of the heat transfer in a tube bundle with the pulsating flow is needed.

Acknowledgments

The article is executed within the framework of the scientific project 18-79-10136 «Theoretical methods for modeling and developing energy-efficient import-substituting cleaners and deep processing of hydrocarbon raw materials at enterprises of the fuel and energy complex».

References

- [1] Zukauskas A, Makarevicius V and Slanciauskas A 1968 *Heat transfer in Banks of tube in crossflow of fluid* (Vilnius: Mintis) p 192
- [2] Zukauskas A 1987 *Advan. In Heat Trans.* **18** 87
- [3] Balabani S and Yianneskis M 1996 *Proc. IMechE Part C: J. Mech. Eng. Sci.* **210** 317
- [4] Wang Y Q, Penner L A and Orm S J 2000 *Numer. Heat Tr. A-Appl.* **38** 819
- [5] Gorobets V, Bohdan Y, Trokhaniak V and Antypov I 2019 *Appl. Therm. Eng.* **151** 46
- [6] Gorman J M, Sparrow E M and Ahn J 2019 *Int. J. Heat Mass Tran.* **132** 837
- [7] Zhao T S and Cheng P 1998 *Annual Rev. Heat Trans.* **9** 359
- [8] Konstantinidis E, Castiglia D, Balabani S 2005 *Proc. IMechE Part C: J. Mech. Eng. Sci.* **219** 283
- [9] Konstantinidis E, Balabani S, Yianneskis M 2003 *Trans IchemE Part A.* **81** 695
- [10] Konstantinidis E, Castiglia D, Papadakis G Balabani S and Bergeles G 2000 *10th Int. Symp. Appl. Laser Tech. Fluid Mech.* **1**
- [11] Konstantinidis E, Balabani S and Yianneskis M 2002 *ASME J. Fluids Eng.* **124** 737
- [12] Liang C and Papadakis G 2005 *Eng. Turb. Mod. and Exp.* **6** 813

- [13] Molochnikov V M, Mikheev N I, Vazeev T A and Paereliy A A 2017 *J. Phys.: Conf. Ser.* **891** 012049
- [14] Molochnikov V M, Mikheev A N, Aslaev A K, Goltsman A E and Paereliy A A 2018 *J. Phys.: Conf. Ser.* **1105** 012024
- [15] Aslaev A K, Mikheev A N, Molochnikov V M, Goltsman A E and Paereliy A A 2018 *7th Russian National Conf. Heat Trans.* 300
- [16] Molochnikov V M, Mikheev A N, Aslaev A K, Dushina O A and Paereliy A A 2019 *Therm. and Aeromechanics* **26** 519
- [17] Ilyin V K, Sabitov L S, Haibullina A I and Hayrullin A R 2017 *IOP Conf. Ser.: Mater. Sci. Eng.* **240** 012027
- [18] Ilyin V K, Sabitov L S, Haibullina A I and Hayrullin A R 2017 *IOP Conf. Ser.: Mater. Sci. Eng.* **240** 012026
- [19] Ilyin V K, Sabitov L S, Haibullina A I and Hayrullin A R 2017 *IOP Conf. Ser.: Mater. Sci. Eng.* **240** 012025
- [20] 2011 *Ansys Fluent* (ANSYS Inc.: Southpointe)